Biosensors and Bioelectronics 105 (2018) 90–94

Contents lists available at ScienceDirect

Biosensors and Bioelectronics

journal homepage: www.elsevier.com/locate/bios

Ultrasensitive sensor for detection of early stage chronic kidney disease in human

Dignya Desai[a,b], Ashok Kumar[b,*], Debajyoti Bose[c], Manali Datta[a,*]

[a] Amity Institute of Biotechnology, Amity University Rajasthan, 303007, India
[b] CSIR-Institute of Genomics and Integrative Biology, Mall Road, Delhi 110007, India
[c] Department of Biological Science, Yobe State University, Nigeria, Africa

ARTICLE INFO

Keywords:
Chronic kidney disease
Papain
Cystatin C
CKD sensor

ABSTRACT

A facile label free, ultrasensitive platform for a rapid detection of chronic kidney disease has been fabricated. Early intervention in patients with chronic kidney disease has the potential to delay, or even prevent, the development of end stage renal disease and complications, leading to a marked impact on life expectancy and quality of life. Thus, a potable electrochemical diagnostic biosensor has become an attractive option as electrochemical analysis is feasible to use for on-site detection of samples. In human, Cystatin C present in human body fluids is freely filtered by the glomerulus, but reabsorbed and catabolised by the renal tubules. Trace detectable amount is eliminated in urine, giving this molecular marker an edge over serum creatinine's disadvantages. A carboxyl functionalized multiwalled carbon nanotubes screen printed electrode was immobilized with papain (cysteine protease) where amino group of papain covalently bound carboxyl group on electrode surface by EDC (1-ethyl-3-(3-dimethylaminopropyl) carbodiimide) and NHS (N-hydroxysuccinimide) chemistry. The modifications on sensor surface were characterized by field emission scanning electron microscopy. Interaction between papain and chronic kidney disease specific biomarker, Cystatin C was detected by cyclic voltammetry and differential pulse voltammetry within 10 min. The sensor is highly specific to Cystatin C and showed negligible response to non-specific macromolecules present in urine. The sensitivity of the sensor was 1583.49 $\mu A\ cm^{-2}\ \mu g^{-1}$ and lower limit of detection of Cystatin C was found 0.58 $ng\ L^{-1}$ which presents as a promising platform for designing potable kidney disease detector.

1. Introduction

Chronic kidney disease (CKD) is the fourth most common non-communicable form of kidney malfunction, characterized by progressive loss of function of the renal tubules. Increasing evidences have established CKD to be a secondary syndrome associated with lifestyle disorders like hypertension, cardiovascular disease, diabetes and hormonal imbalances (Bello et al., 2005) with a prevalence rate of 1 in every 10 adults. Additionally, it has been observed that CKD as a preliminary manifestation may eventually lead to hormonal imbalances, thus making it a part of 'vicious cycle' (Thomas et al., 2008). Progression of CKD is categorized in stages I-V demarcated by the changes in glomerular filtration rate (eGFR < 60 mL min^{-1} 1.73 m^{-2}) and proteinuria (30 mg g^{-1} or higher) (Biljak et al., 2017; Almeida et al., 2015; Ghaderian and Beladi-Mousavi, 2014). Hospital based detection are tedious and currently possible for stage III-V CKD patient. Inability to curb the progression of CKD leads to acute kidney failure (stage V) (Neild, 2017) and mortality becomes a confirmed likelihood as administration of therapy (angiotensin inhibitors) is delayed (Biela, 2015; Levey et al., 2005). At present, there is a dearth of diagnostics that detect CKD patients at stages I and II using non invasive samples. Hence, the necessity arises to develop facile diagnostics for candidates destined for CKD progression.

Although, several biomarkers are reported for CKD such as creatinine (Cr), neutrophil gelatinase-associated lipocalin (NGAL), kidney injury molecule-1 (KIM-1), liver-type fatty acid binding protein (L-FABP) and Cystatin C (CysC), CysC has been identified as the most decisive "gold standard marker" for CKD progression (Uchida and Gotoh, 2002). CysC, a cysteine protease inhibitor, has been established as a constituent of urine of normal individual and has a tendency to be reabsorbed by healthy kidneys (Kazuo and Akiko, 2002). Elevated levels of CysC is innately associated with disease prognosis. As per CKD-EPI equation, CysC has been found to be statistically correlated with increasing Cr concentration and decreasing eGFR signifying deteriorating kidney functionality. Additionally, CysC is devoid of its association with variation in age, sex and dietary intake of individuals as

* Corresponding authors.
E-mail addresses: ashok@igib.res.in (A. Kumar), manali.datta@gmail.com (M. Datta).

https://doi.org/10.1016/j.bios.2018.01.031
Received 5 October 2017; Received in revised form 11 January 2018; Accepted 15 January 2018

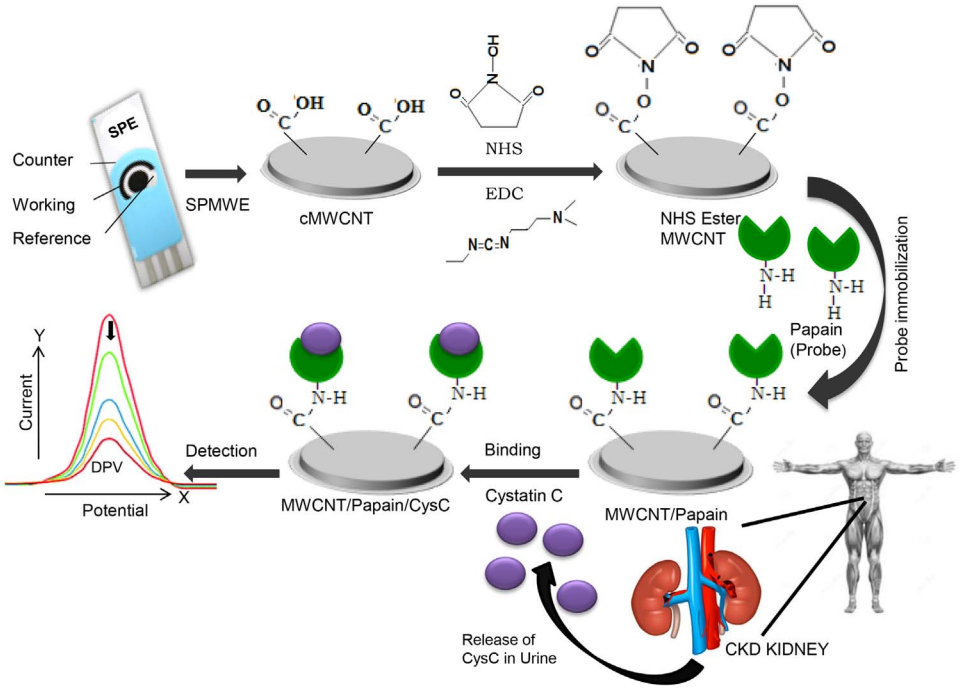

Scheme 1. Schematics of non-invasive strategy for detection of CKD biomarker CysC in human urine. Papain covalently immobilized on working surface of carboxyl activated SPMWE using EDC:NHS chemistry. SPMWE incubated with increasing concentration of CysC for 10 min at RT (27° C) was measured by electrochemical methods using 5 mM of potassium ferricyanide [$K_3[Fe(CN)_6]$] as indicator at pH 7.2. Electrochemical response of probe (SPMWE/papain) with CysC was measured by CV (−200 V to 800 V) and DPV (−400 to 600 mV).

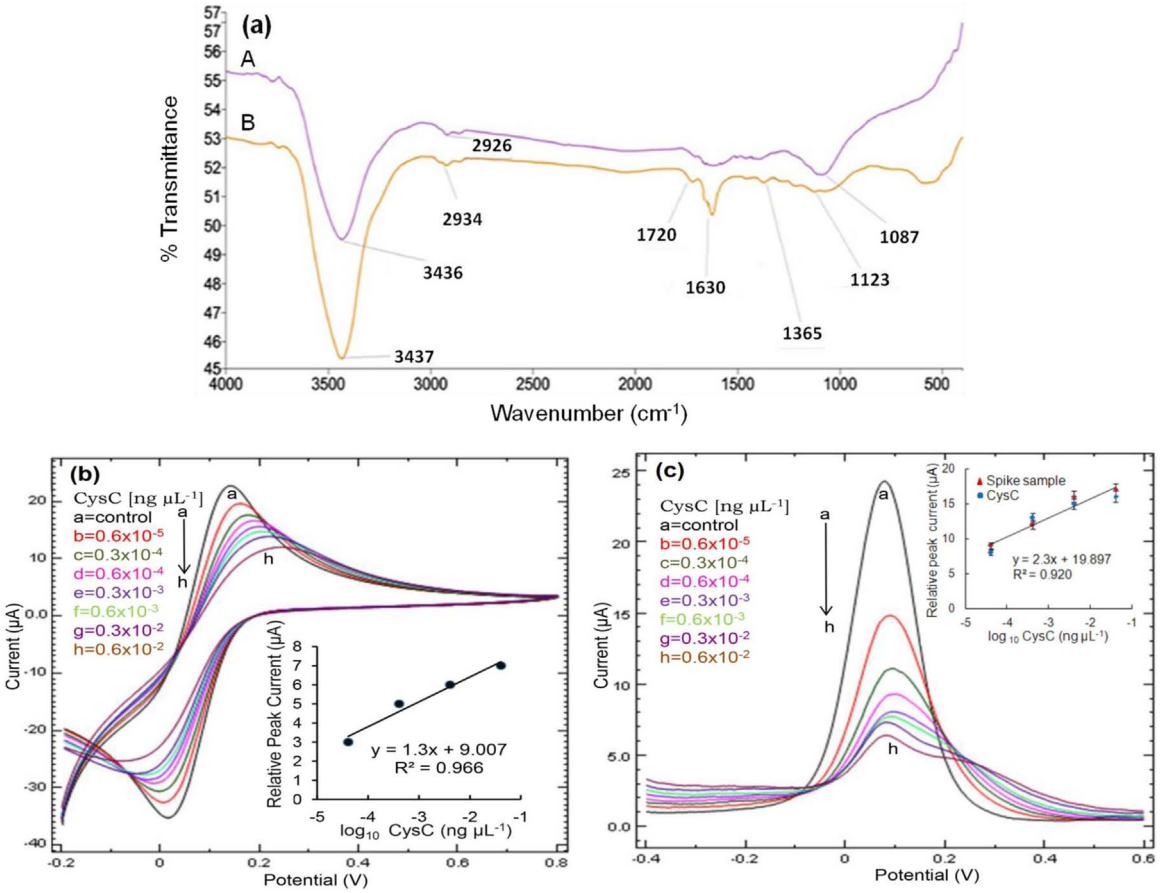

Fig. 1. (a) FTIR spectra of [A] cMWCNT and [B] MWCNT/papain for confirmation of covalent linkage between MWCNT and papain through amide bond using EDC-NHS chemistry at frequency 400–4000 cm^{-1}. **(b)** Electrochemical CV response study using 5 mM $K_3[Fe(CN)_6]$ in 0.1 M PB, pH 7.2, CV of SPMWE/papain as control (a) and binding with 0.6×10^{-5} ng μL^{-1} to 6.6×10^{-3} ng μL^{-1} CysC (b→h). [Inset] Plot shows relationship between relative I_p with lowest concentrations of CysC, where X-axis is relative peak current (µA) and Y-axis is $\log_{10}$ concentration (CysC). **(c)** DPV plot of biosensor using different CysC concentrations ranging from 0.6×10^{-5} ng μL^{-1} to 6.6×10^{-3} ng μL^{-1}. [Inset] Plot shows relationship between different concentration of CysC for the calculation of sensitivity and LOD, where X-axis is relative peak current (µA) with respect to control (SPMWE/papain) and Y-axis is CysC concentration in $\log_{10}$.

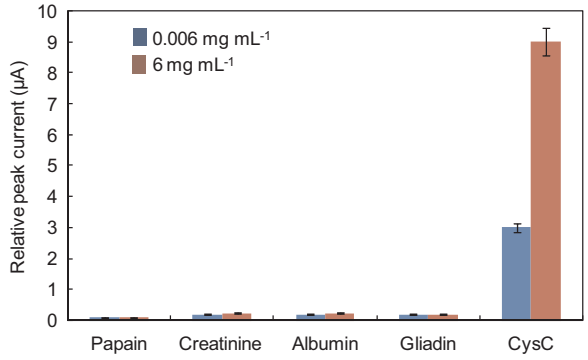

Fig. 2. Specificity of the CKD sensor was detected using DPV with CysC and other possible macromolecules present in urine. Two concentrations of CysC and other macromolecules (0.006 mg mL^{-1} and 6 mg mL^{-1}) were measured in the range of −400 to 600 mV. Three readings were taken for each macromolecule at same conditions.

opposed to other biomarkers for CKD (Shlipak et al., 2006; Grubb et al., 2005). CysC based diagnostics have been designed (Gorodkiewicz and Luszcyn, 2011; Lars-Olof et al., 2010), but the methods are time consuming, expensive, tedious and requires trained manpower and sophisticated equipments, which may not be present universally. Biosensors are ultrasensitive devices, categorized on the basis of transducer types namely electrochemical, colorimetric, fluorescence, piezoelectric, etc (Datta et al., 2017). Electrochemical biosensors have become an attractive option for high throughput analysis combined with advantages of easy handling, enhanced sensitivity, high selectivity, and rapidity of data collection (Grabowska et al., 2014; Govindhan et al., 2014). As of date no sensor has been designed to detect marker based non symptomatic CKD. Screen printed electrodes provide an inexpensive and handy electrochemical platform as opposed to bulky glassy electrodes.

With the advent of nanotechnology, huge opportunities have arisen to improve the sensitivity, stability and specificity of sensor technology. Carbon nanotubes (CNT) as a transducer in electrochemical biosensors mediates an efficient electron transfer between the immobilized probe, especially proteins and electrode (Sharma et al., 2009; Harris, 2004: Iijima, 1991; Nugent et al., 2001; Arvinte et al., 2008). The architecture of multiwalled CNTs provides a high surface area thus enabling increased probe loading and efficient electron transfer kinetics (Hegde et al., 2011; Tu et al., 2005; Doubnerova and Ryslava, 2011).

Here, we report a nanosensor for detection of early stage CKD. Screen printed multiwalled carbon nanotube (MWCNT) electrode immobilized with papain was devised as a working control electrode. Specificity of papain as capture molecule was employed to bind the CKD biomarker CysC (Lalmanach et al., 1993). Protein-protein interaction mediated transduction of electrons (Nocek et al., 1996) by the modified SPMWE/papain was measured through cyclic voltammetry (CV) and differential pulse voltammetry (DPV). Our designed platform was further investigated for specificity. Superiority of the electrochemical CKD sensor was confirmed on comparison with other available techniques in terms of specificity, sensitivity and limit of detection (LOD), thus opening new opportunities for CKD detection in state of art efficient clinical diagnosis.

2. Experimental

2.1. Materials

SPMWE-COOH (cMWCNT)/ carbon electrode REF: C110CNT was purchased from Dropsens, Spain and modified at IGIB. Papain, Cystatin C (CysC), 1-Ethyl-3-(3-dimethyl-aminopropyl) carbodiimide (EDC) and *N*-hydroxysuccinimide (NHS) were purchased from Sigma Aldrich, USA. Potassium hexacyanoferrate (III) [$K_3Fe(CN_6)$], Ethanol and other chemicals were obtained from Qualigens, India. All other reagents were analytical grade and solutions were prepared in phosphate buffer, pH 7.2 (PB).

2.2. Fabrication of functionalized electrode

Screen printed cMWCNT electrode (SPMWE) (4.0 mm diameter) was purchased from Dropsens, modified in lab, and used as a template for immobilization of the probe (papain). SPMWE was washed two times with autoclaved Milli-Q water and 0.01 mM phosphate buffer, pH 7.2 (PB) and was dried at room temperature (RT 27 °C). Reactive ester groups were generated on electrode by incubating a mixture of 10 mM EDC and 10 mM NHS (1:1, v/v in PB) for 1 h. Excess reagent was washed off using buffer and electrode was dried at RT (Kaushal et al., 2017). The functionalized electrode thus designed, was incubated with 6 μL of papain solution (5 mg mL^{-1}) for three hours at RT followed by repeated buffer washing. Excess unbound papain in washout was analyzed at 280 nm using Nanodrop spectrophotometer (ND-1000 Thermo Scientific).

2.3. Mechanism of sensing

The mechanism of sensing of CysC in the sample is represented in Scheme 1. The different parameters such as interaction time of papain with CysC and temperature were optimized for electrochemical study of the sensor (Tables S1 and S2). Binding of the targeted biomarker to probe leads to induction of an electronic signal. CV and DPV measurements were conducted using 5 mM potassium ferricyanide [$K_3Fe(CN_6)$] as the redox indicator. Different concentrations of CysC (0.6×10^{-5}–6.6×10^{-3} ng μL^{-1}) were used to monitor the fluctuations in electronic transitions. In order to test the platform's potential for in-situ urine testing, samples were collected from healthy volunteers for analysis and measurements were observed for both control and spiked sample at concentration varying between 0.6×10^{-5} ng μL^{-1} and 6.6×10^{-3} ng μL^{-1}.

Some other biomarkers like Cr, albumin and gliadin were tested to identify the cross-reactivity of the sensor platform. Test solutions (0.006 mg mL^{-1}) for Cr and albumin and gliadin were prepared in PB. 6 μL of test solution of Cr was incubated with SPMWE/papain for 10 min at RT followed by buffer washing. Post drying, electrochemical measurements at −400–600 mV (FRA 2, μAUTOLAB, Type 3) were

Table 1
Comparison of different methods available for detection of CysC.

S. no	Detection methods	Limit of detection (mg L^{-1})	Detection time (Min)	References
1	PENIA (Siemens)	0.53–0.95	6	Lars-Olof et al. (2010)
2	PETIA (COBAS)	0.47–1.09	10	Lars-Olof et al. (2010)
3	PETIA (Genzyme)	0.61–1.17	10	Stephen et al. (2017)
4	MWCNT diagnostics	0.5–5.0	30	Stephen et al. (2017)
5	SPRI sensor	0.09	10	Gorodkiewicz and Luszcyn (2011)
6	SPMWE sensor	0.006	10	Present

PENIA: Particle enhanced nephelometric assay; PETIA: Particle enhanced turbidimetric assay; MWCNT: Multiwalled carbon nanotubes; SPRI: Surface Plasmon Resonance Imaging; SPMWE: Screen printed MWCNT electrode.

taken. Similarly, all the selected biomarkers were tested on the different working electrodes with above mentioned protocol and the change in current was measured by DPV as described above.

2.4. Characterization of working electrode (SPMWE)

The surface topography of bare (cMWCNT) and papain immobilized (MWCNT/Papain) was carried out by Fourier transform infrared spectroscopy (FTIR) at frequency range 400–4000 cm^{-1} (PerkinElmer Spectrum Version 10.4.00).

3. Results and discussion

3.1. Characterization of working electrode

The FTIR spectra were taken as control (SPMWE) and after immobilization of papain through EDC-NHS chemistry for confirmation of covalent linkage of papain to carboxylated multiwalled carbon nanotubes [Fig. 1(a)]. The spectrum [A] shows the transmittance of the MWCNT electrode at different wave number. The presence of carboxyl activated MWCNTs could be determined by peak at 3436 cm^{-1} and 2926 cm^{-1} corresponding to the O–H stretch from carboxyl groups (O=C−OH and C−OH), with rest peak at 1087 cm^{-1} for C=O stretch. The spectrum [B] shows amide bond formation between -NH2 groups of papain and -COOH groups of MWCNT was determined by the presence of peak at 1720 cm^{-1} and 1630 cm^{-1} along with peak at 1365 cm^{-1} resembling C-C stretch, C=O stretch, C-H bend and N-H stretch with rest peak 1123 cm^{-1} for C=O (ester) and C-O stretching and vibrations. The binding of papain with CysC is already established in protein-protein interaction (Lalmanach et al., 1993).

3.2. Electrochemical study of biosensor

Working electrode was studied by CV and DPV in 5 mM $K_3[Fe(CN)_6]$ solution in buffer as redox indicator at potential range from −200V to 800 V for CV and −400–600 mV for DPV with scan rate 10 mV s^{-1}. The peak current (I_P) of control was found to be 23 μA for CV and 24 μA for DPV. CV and DPV Ip of bare SPMWE is greater than the CV and DPV Ip of SPMWE/papain due to more conductivity in SPMWE electrode than SPMWE/papain. The CV I_p of probe (SPMWE/papain) electrode was taken as control (23 μA) for analyzing the effect of various CysC concentrations prepared in PB [Fig. 1(b)]. The I_p of SPMWE/papain/CysC was lower than that of SPMWE/papain and it reduced with increasing concentrations of CysC as electrons were channelized in protein-protein interaction. The plot between the various concentrations of CysC and the relative I_p values with reference to the probe was hyperbolic for CysC following a linear equation [Ip (μA) = 1.3 (μA ng^{-1}) × CysC (ng) + 9.007] with good correlation (regression coefficient R^2 = 0.966) [Fig. 1(b), inset] The sensitivity (S) of the CysC sensor was 158.33 μA cm^{-2} ng^{-1}, calculated using the formula, S = m/A, where, m is the slope of the linear equation and A is the area of the working SPMWE (0.126 cm^2). The limit of detection (LOD) was calculated using the formula LOD = 3 (σ/S) where, σ is the standard deviation and S is the sensitivity (Dash et al., 2013; Bhatnagar et al., 2017; Kaushal et al., 2017). The limit of detection (LOD) for CysC was found 0.6 × 10^{-4} mg L^{-1} (60 ng L^{-1}).

In DPV measurements, with increase in CysC concentrations, consistent dip in the current was observed. For CysC concentrations namely, 0.6 × 10^{-5} ng μL^{-1}, 0.3 × 10^{-4} ng μL^{-1}, 0.6 × 10^{-4} ng μL^{-1}, 0.3 × 10^{-3} ng μL^{-1}, 0.6 × 10^{-3} ng μL^{-1}, 0.3 × 10^{-2} ng μL^{-1} and 0.6 × 10^{-2} ng μL^{-1}, the observed peak currents were 15 μA, 11 μA, 9 μA, 8 μA, 8 μA, 7 μA and 6 μA respectively. With increase in the concentration of CysC, corresponding decrease in the current response was recorded with $K_3[Fe(CN)_6]$ solution on the electrode surface [Fig. 1(c)]. For CysC following a linear equation, [Ip (μA) = 2.3 (μA ng^{-1}) × CysC (ng) + 19.897] with good correlation (regression coefficient R^2 = 0.920) (Bhatnagar et al., 2017; Singh et al., 2017). For calculation of S and LOD, the concentrations of control as zero (0), 0.6 × 10^{-5} ng μL^{-1}, 0.3 × 10^{-4} ng μL^{-1} 0.6 × 10^{-4} ng μL^{-1} and 0.3 × 10^{-3} ng μL^{-1}, CysC were considered to achieve best regression coefficient of 0.920. The DPV I_P of SPMWE/papain/CysC was lower than that I_P of SPMWE/papain and it decreases with increasing concentrations of CysC due to protein-protein interaction. The plot between the various concentrations of CysC and the relative I_p values with reference to the probe was hyperbolic. The sensitivity (S) and LOD was calculated using same formula used in CV measurement. The S of the designed CKD sensor was 1583.49 μA cm^{-2} μg^{-1} and LOD was found approximately 5.8 × 10^{-6} mg L^{-1} (0.58 ng L^{-1}).

3.3. Specificity and stability study of the sensor

The plausible cross-reactivity of the sensor with other possible macromolecules (creatinine, albumin, gliadin) found in urine were tested (Fig. 2). The I_p of the sensor with CysC and with other biomarkers present in urine were found approximately same as immobilized probe (papain) except with CysC. The specificity of the sensor was tested using DPV. The Ip of the sensor after 10 min incubation with non-specific biomarkers was found to be almost same. In contrast, CysC demonstrated consistent reduced I_p even after 20 min incubation. This may be attributed to the stable binding of CysC with papain (Grzonka et al., 2001) (association constant equal to 5.5 × 10^{-7} mol^{-1} s^{-1}) (Bjork et al., 1989). As significant reduction in I_p value was evident only in CysC, selectivity and specificity for the targeted CKD biomarker could be ascertained. The stability of the CKD sensor was also studied by measuring the change in DPV current at every month on storage at 4 °C (Fig. S1, Supplementary Information). The sensor was found to be stable for 12 months with only 10% approximate loss in initial I_p value on storage at 4 °C.

4. Conclusion

It is first time an ultrasensitive protein-protein interaction based SPMWE sensor has been designed for highly sensitive detection of CKD at stages I and II using non- invasive samples. Biosensor designed is based on principle of protein-protein interaction and electrochemical method. Literature cites normal CysC level in urine ranges from 100 μg L^{-1} and tends to increase 200 fold with kidney malfunction. A comparative study was carried out to identify the significance of the fabricated sensor (Table 1). A previously designed SPRI sensor could detect up to 0.09 mg L^{-1} levels of CysC in serum, but it was very tedious and not user friendly. Another diagnostic developed could detect the stages I and II of CKD, but had an elevated response time. The present ultrasensitive and rapid point-of-care technique (POCT) is capable of detecting CKD with minimal volume (6 μL) and time (10 min) with a diminutive detection limit 5.8 × 10^{-6} mg L^{-1} (0.58 ng L^{-1}) and with the sensitivity of 1583.49 μA cm^{-2} μg^{-1}. The developed POCT is economical and efficient, when compared with other present methods for detection of CKD like previously validated nephelometric assay (PENIA) or performance of the turbidimetric assay (PETIA) systems and hence, it may serve as a fruitful diagnostic for the prevention of progressive CKD.

Acknowledgments

Authors acknowledge Dr S. S. Islam and Mr. Talib for HR-FESEM images at Jamia Millia Islamia University, New Delhi and Mr. Sourabh Sharma for FTIR at MNIT Jaipur, Rajasthan. This research did not receive any specific grant from funding agencies in the public, commercial, or not-for-profit sectors.

Appendix A. Supporting information

Supplementary data associated with this article can be found in the online version at http://dx.doi.org/10.1016/j.bios.2018.01.031.

References

Almeida, F.A.D., Ciambelli, G.S., Bertoco, A.L., Jurado, M.M., Siqueira, G.V., Bernardo, E.A., Gianini, R.J., 2015. Cien. Saude Colet. 20, 471–478.
Arvinte, A., Rotariu, L., Bala, C., 2008. Sensors 8, 1497–1507.
Bello, A., Nwankwo, E., Nahas, M., 2005. Kidney Int. 68, S11–S17.
Bhatnagar, D., Kaur, I., Kumar, A., 2017. Biosens. Bioelectron. 95, 505–510.
Biela, C., 2015. J. Ren. Nurs. 7 (185-185).
Biljak, R.V., Honović, L., Matica, J., Krešić, B., Vojak, S., 2017. Biochem. Med. 27, 153–176.
Bjork, I., Alriksson, E., Ylinenjarvi, K., 1989. Biochemistry 28, 1568–1573.
Datta, M., Desai, D., Kumar, A., 2017. Indian J. Microbiol. 57, 139–147.
Doubnerova, V., Ryslava, H., 2011. Plant Sci. 180, 575–583.
Ghaderian, S.B., Beladi-Mousavi, S.S., 2014. J. Ren. Inj. Prev. 3, 109–110.
Govindhan, M., Adhikari, B.R., Chen, A., 2014. Rsc. Adv. 4, 63741–63760.
Gorodkiewicz, E., Luszcyn, J., 2011. Protein Pept. Lett. 18, 23–29.
Grabowska, I., Malecka, K., Jarocka, U., Radecki, J., Radecka, H., 2014. Acta Biochim. Pol. 61, 471–478.
Grubb, A., Nyman, U., Björk, J., Lindström, V., Rippe, B., Sterner, G., Christensson, A., 2005. Clin. Chem. 51, 1420–1431.
Grzonka, Z., Jankowska, E., Kasprzykowski, F., Kasprzykowska, R., Lankiewicz, L., Wiczk, W., Kozak, M., 2001. Acta Biochim. Pol. 48, 1–20.
Harris, P.J.F., 2004. Int. Mater. Rev. 49, 31–43.
Hegde, R.N., Chandra, P., Nandibewoor, S.T., 2011. J. Nanosci. Nanotechnol. 1, 75–86.
Iijima, S., 1991. Nature 354, 56–58.
Kazuo, U., Akiko, G., 2002. Clin. Chim. Acta 323, 121–128.
Kaushal, A., Singh, S., Kumar, A., Kumar, D., 2017. Indian J. Microbiol. 57, 121–124.
Lalmanach, G., Hoebeke, J., Moreau, T., Brillard-Bourdet, M., Ferrer-Di Martino, M., Borras-Cuesta, F., Gauthier, F., 1993. J. Protein Chem. 12, 24–31.
Lars-Olof, H., Anders, G., Anders, L., Mats, F., Annacarin, B., Joris, D.U., Veronique, S.U., Hilmar, L., Karl-Heinz, R., Claus, B., 2010. Scand. J. Clin. Lab. Investig. 70, 347–353.
Levey, A.S., Eckardt, K.U., Tsukamoto, Y., Levin, A., Coresh, J., Rossert, J., Zeeuw, D.D., Hostetter, T.H., Lameire, N., Eknoyan, G., 2005. Kidney Int. 67, 2089–2100.
Neild, G., 2017. Pediatr. Nephrol. 32, 243–248.
Nocek, J.M., Zhou, J.S., De Forest, S., Priyadarshy, S., Beratan, D.N., Onuchic, J.N., Hoffman, B.M., 1996. Chem. Rev. 96, 2459–2490.
Nugent, J.M., Santhanam, K.S.V., Rubio, A., Ajayan, P.M., 2001. Nano Lett. 1, 87–91.
Shlipak, M.G., Katz, R., Sarnak, M.J., Fried, L.F., Newman, A.B., Stehman-Breen, C., Seliger, S.L., Kestenbaum, B., Psaty, B., Tracy, R.P., Siscovick, D.S., 2006. Ann. Int. Med. 145, 237–246.
Sharma, A.K., Vatsyayan, P., Goswami, P., Mintee, S.D., 2009. Biosens. Bioelectron. 24, 2313–2322.
Singh, S., Kaushal, A., Khare, S., Kumar, A., 2017. Int. J. Biol. Macromol. 11, 355–359.
Stephen, B., Desai, D., Datta, M., 2017. Asian J. Pharm. Clin. Res. 10, 425–429.
Thomas, R., Kanso, A., Sedor, J.R., 2008. Prim. Care 35, 329–344.
Tu, Y., Lin, Y., Yantasee, W., Ren, Z., 2005. Electroanalysis 17, 79–84.
Uchida, K., Gotoh, A., 2002. Clin. Chim. Acta 323, 121–128.